

## GENERATION OF STABLE THERMAL STRATIFICATION BY TURBULENT FLOWS IN A PARTIALLY OPEN ENCLOSURE

Abdulkarim H. Abib and Yogesh Jaluria  
Department of Mechanical and Aerospace Engineering  
Rutgers University  
New Brunswick, New Jersey

### ABSTRACT

A numerical study of the turbulent flow induced by the energy input due to a heat source at the bottom boundary in a partially open rectangular cavity is carried out. Such flows are of interest in enclosure flows induced by localized sources such as fires and electronic components. The flow in the open cavity interacts with its surroundings through the opening. Of particular interest is the influence of opening height on the generation of thermal stratification within the cavity. Therefore, the effect of opening height is explored for an isothermal ambient medium using a wide range of Grashof numbers, spanning both laminar and turbulent regimes. A control-volume finite-difference method, a stream function vorticity formulation, is employed for the solution of the initial-value problem. A low Reynolds number  $k - \epsilon$  turbulence model is used for the turbulent flow calculations. This model is particularly suitable for flows in which the possibility for re-laminarization exists.

It was found that, for high Grashof numbers and for relatively small opening heights, particularly for doorway openings, a strong stable thermal stratification is generated within the cavity, with a cooler essentially uniform lower-layer and warmer linearly stratified upper-layer. As a consequence, turbulence is suppressed and the flow in the upper region of the cavity becomes laminar with turbulence confined to isolated places such as the thermal plume above the source and the shear-layer at the opening. The penetration distance and the height of the interface are both found to decrease with a reduction in the opening height. The Nusselt number for heat transfer from the source is seen to be affected to a small extent by the opening height.

### NOMENCLATURE

$A$  aspect ratio,  $A = L/H$   
 $C_{3\epsilon}, C_{\mu}$  empirical constants in the turbulence model

$C_{3\epsilon}, C_{\mu}$  empirical constants in the turbulence model  
 $f_1, f_2, f_{\mu}$  damping wall functions in the turbulence model  
 $Gr$  Grashof number based on the height of the cavity  
 $Gr = g\beta \frac{Q_0}{\alpha} H^3 / \nu^2$   
 $g$  magnitude of the gravitational acceleration  
 $H$  height of the cavity  
 $H_i$  height of the interface  
 $H_0$  height of the opening  
 $h_0$  dimensionless height of the opening,  $H_0/H$   
 $K$  dimensionless turbulent kinetic energy  
 $L$  length of the cavity  
 $L_e$  length of the extended computational domain  
 $L_s$  length of heat source  
 $L_t$  thickness of the doorway soffit  
 $l_e$  dimensionless length of the extended computational domain,  $l_e = L_e/H$   
 $l_s$  dimensionless length of heat source,  $l_s = L_s/H$   
 $l_t$  dimensionless thickness of the doorway soffit,  $l_t = L_t/H$   
 $\dot{m}$  dimensionless mass outflow rate at the opening  
 $\overline{Nu_s}$  average Nusselt number over the source, defined in Eq. (17)  
 $n$  normal distance from nearest wall  
 $Pr$  Prandtl number,  $Pr = \frac{\nu}{\alpha}$   
 $Q_0$  total heat input by the energy source per unit width  
 $Re_n$  local Reynolds number,  $Re_n = \frac{\sqrt{K}n}{\nu}$   
 $Re_s$  local Reynolds number,  $Re_s = \frac{K^2}{\nu \epsilon}$   
 $T$  temperature  
 $t$  dimensionless time

$u, v$	dimensionless mean velocity components in the x and y coordinate directions, respectively
$X$	horizontal coordinate
$X_s$	distance between the source and the back wall
$x$	dimensionless horizontal coordinate, $X/H$
$x_s$	dimensionless distance between the source and the back wall, $x_s = X_s/H$
$Y$	vertical coordinate
$y$	dimensionless vertical coordinate, $Y/H$
$Z_i$	dimensionless height of hot-cold interface

### Greek Letters

$\alpha$	thermal diffusivity
$\beta$	coefficient of thermal expansion, $\beta = \frac{1}{T}$ for perfect gas
$\gamma$	stratification level
$\delta_p$	dimensionless penetration height of the thermal plume
$\epsilon$	dimensionless dissipation of turbulent kinetic energy
$\kappa$	coefficient of thermal conductivity
$\nu$	kinematic viscosity
$\nu_e$	effective eddy diffusivity, $\nu_e = 1 + \nu_t/\nu$
$\nu_t$	turbulent eddy diffusivity
$\rho$	density
$\Delta T_q$	characteristic temperature difference, $\Delta T_q = Q_0/\kappa$
$\Delta t$	dimensionless time step
$\Theta$	dimensionless temperature, $\Theta = \frac{T - T_\infty}{\Delta T_q}$
$\psi$	dimensionless stream function
$\sigma_t, \sigma_k, \sigma_\epsilon$	turbulent Prandtl numbers for $\Theta$ , $K$ , and $\epsilon$ , respectively
$\zeta$	dimensionless vorticity

### Subscripts

$e$	effective value of turbulent eddy diffusivity
$i$	hot-cold interface
$s$	heat source
$w$	wall value

## INTRODUCTION

Buoyancy-induced flows frequently arise from heated surfaces and sources in the presence of other surfaces. Such surfaces may not often collectively form a complete enclosure. For instance, partial enclosures represent heated spaces with open doors or windows, inlet, and outlets. Even in closed rooms, there are often small cracks and openings that allow infiltration of air into the room. The air that enters the room through these openings may then interact with the flow generated within the room. This interaction between the enclosure and the surrounding ambient media is the subject of the present work.

Transport processes in partial enclosures are very different from those in similar completely closed enclosures. They are usually strongly dependent on the nature, size, location and number of openings or vents, as well as on the temperature distribution in the ambient medium. The effect of venting or entrainment of air on the growth of a fire and on the removal of combustion gases from the enclosure is very important and is well recognized (Quintiere 1977, 1984). In fact, in a developing fire, venting controls the temperature and heat transfer, thereby influencing the spread of the fire. In a fully developed fire, the rate of inflow of air controls the rate of fuel combustion. Therefore, it is important to study the interaction between the enclosure and the surroundings through the opening in order to describe these flows correctly in mathematical models which simulate fire growth in enclosures. Similar considerations arise in the cooling of electronic components located in enclosed spaces.

The study of natural convection flows arising from localized or volumetric energy sources located at the bottom in a partially open enclosure has received considerable attention in the last 30 years and include the papers by Kawagoe (1958), Ku et al. (1976), Emmons (1978), Steckler et al. (1982), Markatos et al. (1982), Satoh et al. (1983, 1984) and many others.

The work done by Kawagoe (1958) dealt with a fully-developed fire situation in a room which was assumed to be at a uniform temperature. The buoyancy-driven gas flow through the doorway or window opening was treated as an orifice flow problem. A flow coefficient of 0.7, taken from pipe flow technology, was assumed to be valid for these openings. The orifice concept was carried over to the zone model for a developing fire by Thomas et al. (1967), who developed a two-layer model for gas flow through a roof vent, and by Emmons (1973, 1978), Rockett (1976), Zukoski (1975), and Zukoski & Kubota (1978), who modeled the doorway and window-opening versions of the problem. Here again, a flow coefficient of 0.7 was employed.

Steckler et al. (1982) have shown that the vent flows through doors or windows can be computed with good accuracy from careful temperature measurements, provided a flow coefficient is known. The flow coefficient was found to be  $0.7 \pm 0.03$  for a wide range of conditions (Steckler et al., 1984). The results are consistent with the high Reynolds number results of Prah & Emmons (1975) who carried out an analog study using water and kerosene.

Ku et al. (1976) developed a numerical model for the prediction of unsteady two-dimensional buoyant flows in enclosures. They considered a heated room with a corridor. In one case, only the heat source in the room is activated and in the other case, only the heat source in the corridor is turned on. In the first case, the flow pattern exhibited a strong ceiling jet, a cold floor jet in the corridor and a large recirculation region in the room. The thermal plume above the heat source is drawn towards the back side wall. In the second case, the cold floor jet does not penetrate into the room. They also studied the case of a single heated enclosure with an exit doorway. The velocity field exhibits a four-

ver behaviour. They also found that the four-layer effect is sensitive to opening size; the smaller the opening the more pronounced is the four layer structure. Their computations also show that the circulation region is not stationary.

Satoh et al. (1983) carried out 2-D and 3-D turbulent flow numerical calculations to study the oscillatory behaviour of the flow and temperature fields in a square compartment with floor and ceiling vents. A volumetric heat source located either at the center of the floor or at the lower left corner of the compartment was used to simulate the fire. In their computation, an algebraic eddy viscosity turbulence model for recirculating buoyant flows was employed. They found that long-time oscillatory behaviour is prevalent in those cases where the heat source was located at the center of the floor of the compartment. For the cases with the heat source at the corner, the oscillations were found to damp out. Furthermore, they found that the oscillatory motion was not sensitive to the eddy viscosity model.

Markatos et al. (1982) reported a computational procedure for predicting 2-D turbulent smoke movement in a partially open enclosure containing a fire source. A  $k - \epsilon$  turbulence model was employed and the effects of buoyancy on turbulence were included in the model. The results were shown to be in reasonable agreement with experimental data. This work was further extended to a 3-D transient model by Markatos & Cox (1982) and Simcox et al. (1989).

The results for partially open enclosures with internally generated stable thermal stratification, in an isothermal ambient media, are essentially non-existent. Therefore, the primary objective of the present study is to investigate, in detail, the interaction between the partially open enclosure with a localized energy source at the bottom boundary and the surrounding ambient media. The study explores the effect of opening size or height at various Grashof numbers  $Gr$  spanning both laminar and turbulent flows. Furthermore, a comparison between the case with an internally generated stable thermal stratification and the case in which a stable ambient thermal stratification is imposed through the opening is made in order to examine the similarities and differences between the two cases. The effort is mainly directed at determining the heat transfer rate, mass flow rate, the penetration distance of the thermal plume rising above the energy source, and the turbulence and stratification levels that are generated within the cavity, in order to characterize the resulting penetrative and recirculating flow. This problem applies to enclosure fires, electronic cooling as well as other cases.

## ANALYSIS

A numerical study of the turbulent penetrative and recirculating flow due to energy input at the bottom boundary of a partially open rectangular cavity of height  $H$  and aspect ratio (height to length)  $A$  of 2, typical of room-size enclosures, is carried out. This flow is of particular interest in the simulation of flows induced by room fires which was the motivation for this work. A rectangular cavity with an opening is connected to a very long corridor which is

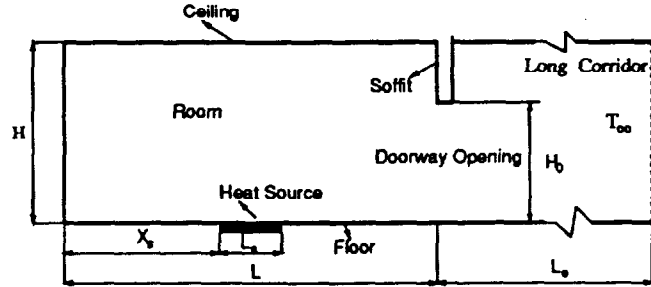


Figure 1: A partially open enclosure heated at the bottom boundary by a localized energy source.

initially in an isothermal conditions as shown in Fig. 1. A single doorway opening is examined since the effect of multiple openings is less significant than that of the opening size, as far as growth and flashover potential of fire is concerned (Quintiere, 1981).

For the present study, the energy source is a localized heat source with a constant heat input per unit width,  $Q_0$ . The role of thermal radiation in the gases is ignored and the focus is on convective flow and transport since interest lies in regions far from the energy source. This is a reasonable approximation for  $Gr < 10^{13}$ . Adiabatic boundary conditions are considered at the side walls, the floor and the ceiling, assuming that these have heated up and are well-insulated.

## Governing Equations

Using  $H$ ,  $\Delta T_q$ , and  $H/\sqrt{g\beta\Delta T_q H}$  as reference length, temperature, and time scales, respectively, the governing equations, in dimensionless form, expressing conservation of mass, momentum, energy, and the turbulent kinetic energy and its dissipation, for an incompressible Boussinesq fluid, can be written as:

$$u = \frac{\partial \psi}{\partial y}; \quad v = -\frac{\partial \psi}{\partial x} \quad (1)$$

$$\frac{\partial^2 \psi}{\partial x^2} + \frac{\partial^2 \psi}{\partial y^2} = -\zeta \quad (2)$$

$$\frac{\partial \zeta}{\partial t} + \frac{\partial(u\zeta)}{\partial x} + \frac{\partial(v\zeta)}{\partial y} = \frac{1}{\sqrt{Gr}} \left\{ \frac{\partial}{\partial x} \left( \frac{\partial(v_e \zeta)}{\partial x} \right) + \frac{\partial}{\partial y} \left( \frac{\partial(v_e \zeta)}{\partial y} \right) \right\} + S_\zeta \quad (3)$$

$$\frac{\partial \Theta}{\partial t} + \frac{\partial(u\Theta)}{\partial x} + \frac{\partial(v\Theta)}{\partial y} = \frac{1}{Pr\sqrt{Gr}} \left\{ \frac{\partial}{\partial x} \left( \nu_{e,\theta} \frac{\partial \Theta}{\partial x} \right) + \frac{\partial}{\partial y} \left( \nu_{e,\theta} \frac{\partial \Theta}{\partial y} \right) \right\} \quad (4)$$

$$\frac{\partial K}{\partial t} + \frac{\partial(uK)}{\partial x} + \frac{\partial(vK)}{\partial y} = \frac{1}{Pr\sqrt{Gr}} \left\{ \frac{\partial}{\partial x} \left( \nu_{e,k} \frac{\partial K}{\partial x} \right) + \frac{\partial}{\partial y} \left( \nu_{e,k} \frac{\partial K}{\partial y} \right) \right\} + P + G - \epsilon \quad (5)$$

$$\frac{\partial \epsilon}{\partial t} + \frac{\partial(u\epsilon)}{\partial x} + \frac{\partial(v\epsilon)}{\partial y} = \frac{1}{Pr\sqrt{Gr}} \left\{ \frac{\partial}{\partial x} \left( \nu_{e,\epsilon} \frac{\partial \epsilon}{\partial x} \right) + \frac{\partial}{\partial y} \left( \nu_{e,\epsilon} \frac{\partial \epsilon}{\partial y} \right) \right\} + \frac{\epsilon}{K} \{ C_{1\epsilon} f_1 (P + C_{3\epsilon} G) - C_{2\epsilon} f_2 \epsilon \} \quad (6)$$

where  $S_\zeta$  is the source term for the mean vorticity equation, given by

$$S_\zeta = \frac{\partial \Theta}{\partial x} + \frac{1}{\sqrt{Gr}} \left\{ 2 \left( \frac{\partial u}{\partial y} \right) \frac{\partial^2 \nu_e}{\partial x^2} - 2 \left( \frac{\partial v}{\partial x} \right) \frac{\partial^2 \nu_e}{\partial y^2} + 4 \left( \frac{\partial v}{\partial y} \right) \frac{\partial^2 \nu_e}{\partial y \partial x} \right\} \quad (7)$$

and  $G$  and  $P$  are buoyancy and shear production of the turbulent kinetic energy, defined as

$$G = -\frac{1}{\sqrt{Gr}} \frac{\nu_i^*}{\sigma_t} \frac{\partial \Theta}{\partial y} \quad (8)$$

$$P = \frac{\nu_i^*}{\sqrt{Gr}} \left\{ \left( \frac{\partial u}{\partial y} + \frac{\partial v}{\partial x} \right)^2 + 2 \left( \frac{\partial u}{\partial x} \right)^2 + 2 \left( \frac{\partial v}{\partial y} \right)^2 \right\} \quad (9)$$

with

$$\nu_i^* = \frac{\nu_i}{\nu} = \sqrt{Gr} f_\mu C_\mu \frac{K^2}{\epsilon} \quad (10)$$

Here  $\nu_e$ ,  $\nu_{e,\theta}$ ,  $\nu_{e,k}$ , and  $\nu_{e,\epsilon}$  are the effective turbulent diffusivities defined as

$$\nu_e = 1 + \nu_i^* ; \quad \nu_{e,\theta} = 1 + \frac{Pr \nu_i^*}{\sigma_t} \quad (11)$$

$$\nu_{e,k} = 1 + \frac{\nu_i^*}{\sigma_k} ; \quad \nu_{e,\epsilon} = 1 + \frac{\nu_i^*}{\sigma_\epsilon} \quad (12)$$

The damping wall functions  $f_1$ ,  $f_2$ , and  $f_\mu$  for the modified low-Reynolds ( $k-\epsilon$ )-model of Lam Bremhorst (see Davidson 1990), here-after denoted as MLB, are:

$$f_1 = 1 + \left( \frac{0.14}{f_\mu} \right)^3$$

$$f_2 = [1 - 0.27 \exp(-Re_t^2)] [1 - \exp(-Re_n)]$$

$$f_\mu = \exp \left\{ -\frac{3.4}{(1 + Re_t/50)^2} \right\} \quad (13)$$

$$Re_t = \frac{K^2}{\nu \epsilon}$$

$$Re_n = \frac{\sqrt{K} n}{\nu}$$

where  $n$  is the normal distance from the nearest wall.

The coefficients  $C_\mu$ ,  $C_{1\epsilon}$ ,  $C_{2\epsilon}$ ,  $C_{3\epsilon}$ ,  $\sigma_t$ ,  $\sigma_k$ , and  $\sigma_\epsilon$  are empirical constants given in Table 1. These constants are recommended by Launder & Spalding (1974), except for the constant  $C_{3\epsilon}$  in the buoyancy term of the  $\epsilon$ -equation, which is suggested by Rodi (1980) to be close to 1 in vertical boundary layers and close to 0 in horizontal layers. For the present work  $C_{3\epsilon}$  was adopted from Fraikin et al. (1980) as  $C_{3\epsilon} = 0.7/C_{1\epsilon}$ . All the symbols are defined in the nomen-

Table 1: Empirical constants for the ( $k-\epsilon$ )-model recommended by Launder & Spalding (1974).

$C_\mu$	$C_{1\epsilon}$	$C_{2\epsilon}$	$C_{3\epsilon}$	$\sigma_\theta$	$\sigma_k$	$\sigma_\epsilon$
0.09	1.44	1.92	0.7	0.9	1.0	1.3

clature. The governing equations give rise to three dimensionless parameters: the Grashof number  $Gr$ , the Prandtl number  $Pr$ , and the opening height  $h_0$ . Since the fluid considered is air the Prandtl number  $Pr$  is set equal to 0.72. The size of the energy source  $L_s$  is set equal to  $0.2H$  and the location is taken as the center of the cavity ( $X_s = 0.9H$ ). Other values for the source size and location are also considered. But these results are not reported here since the main focus is on the influence of the opening height.

### Initial and Boundary Conditions

The initial and boundary conditions for the governing equations (1) - (6) are specified as

- Initial condition at  $t < 0$ :

Isothermal room and environment ( $\Theta = 0$ ). Laminar  $u$ -,  $v$ -,  $\psi$ -,  $\zeta$ - profiles specified, and non-zero perturbations in  $K$  and  $\epsilon$ , typically:

$$K = 10^{-6}, \quad \nu_i^* = \frac{\nu_i}{\nu} = 10, \quad \epsilon = \sqrt{Gr} C_\mu \frac{K^2}{\nu_i^*} \quad (14)$$

- Boundary conditions at  $t \geq 0$ :

1. Bottom boundary (floor) at  $y = 0$ :

$$u = v = \psi = K = \frac{\partial \epsilon}{\partial y} = 0,$$

$$\zeta = \zeta_w, \quad 0 \leq x \leq x_{max}$$

$$\frac{\partial \Theta}{\partial y} = \begin{cases} 0 & 0 \leq x \leq x_s \\ \frac{1}{l_s} & x_s \leq x \leq x_s + l_s \\ 0 & x_s + l_s \leq x \leq x_{max} \end{cases}$$

2. Ceiling at  $y = 1$  and doorway soffit at  $y = h_0$ :

$$u = v = \psi = K = \frac{\partial \epsilon}{\partial y} = \frac{\partial \Theta}{\partial y} = 0,$$

$$\zeta = \zeta_w, \quad 0 \leq x \leq x_{max}$$

3. Left side wall or back wall at  $x = 0$ :

$$u = v = \psi = K = \frac{\partial \epsilon}{\partial x} = \frac{\partial \Theta}{\partial x} = 0, \\ \zeta = \zeta_w, \quad 0 \leq y \leq 1 \quad (15)$$

4. Door soffit walls at  $x = A$  and  $x = A + l_i$ :

$$u = v = \psi = K = \frac{\partial \epsilon}{\partial x} = 0, \\ \zeta = \zeta_w, \quad \frac{\partial \Theta}{\partial x} = 0, \quad h_0 \leq y \leq 1$$

5. Right far-field boundary at  $x = x_{max}$ :

$$v = \frac{\partial u}{\partial x} = \frac{\partial \psi}{\partial x} = \frac{\partial \zeta}{\partial x} = \frac{\partial K}{\partial x} = \frac{\partial \epsilon}{\partial x} = 0, \\ \left\{ \begin{array}{ll} \Theta = 0 & \text{if } u \leq 0 \quad (\text{inflow}) \\ \frac{\partial \Theta}{\partial x} = 0 & \text{if } u > 0 \quad (\text{outflow}) \end{array} \right. \\ 0 \leq y \leq 1$$

For the wall vorticity  $\zeta_w$ , a first-order finite-difference form is used, which was first given by Thom (1928, cited in Roache 1972), as

$$\zeta_w = -2 \frac{\psi_{w+1} - \psi_w}{\Delta n^2} + O(\Delta n) \quad (16)$$

where  $n$  is the direction normal to wall. This first-order form is usually more stable and gives results very close to those for the higher-order forms (Roache, 1972).

In a partially open enclosure, the difficulties encountered in specifying numerically the appropriate boundary conditions at the outflow has been discussed by Le Quere et al. (1981), Penot (1982), Chan & Tien (1985), and Abib (1992). The approach followed in the present work is based on the use of an extended computational domain outside the opening. It was first given by Kettleborough (1972). The outflow boundary conditions are applied at some distance sufficiently far away from the opening such that a further increase does not significantly alter the results obtained for the flow in the enclosure. The dimensions needed for such an extension beyond the opening are determined numerically. In this work, it was found that an extended computational domain of twice the height of the cavity is sufficient to produce an error of less than 0.1% for the mass outflow rate.

Initially, the cavity and the surrounding environment are considered to be isothermal and quiescent. After the onset of the heat input in the cavity, the environment at the far end of the computational domain ( $x = x_{max}$ ) is assumed to remain isothermal. The initial conditions for Eqs. (5) and (6) can be obtained from non-zero perturbations in  $K$  and  $\epsilon$ . Typical values of  $K_0$  is  $10^{-6}$ ,  $\nu_i^*$  is in the range from 2 to 10 and  $\epsilon_0$  is evaluated as  $Gr^{1/2} C_\mu K_0^2 / (\nu_i^*)_0$ . The values of  $K_0$  and  $(\nu_i^*)_0$  were varied and were found to have a negligible effect on the computed results at these values.

## NUMERICAL SOLUTION

The statistically averaged equations governing the mean-flow quantities are given in Eqs. (1 - 6). Despite the time-averaging, the unsteady terms are kept in the formulation of

the governing equations to account for possible unsteadiness in the transport processes. The time averaging is carried out over a time period that is larger than the time scale of turbulence but smaller than the time scale of the mean motion. In an enclosure, the latter scale is basically determined by the time scale of the internal gravity waves.

The governing equations are discretized with the control-volume based finite-difference method in stream function vorticity formulation. The advection and diffusion terms are discretized with the power-law scheme (Patankar, 1980). The temporal discretization is executed implicitly. A modified version of the low Reynolds number  $k-\epsilon$  model of Lam & Bremhorst (1981) is used in the turbulent flow calculations. This model is particularly suitable for flows in which a potential for re-lamination exists. The solution for  $\Theta$ ,  $\zeta$ ,  $\psi$ ,  $K$ , and  $\epsilon$  is obtained by an iterative procedure at each time step. The details of the numerical scheme used are given by Abib (1992).

## RESULTS AND DISCUSSION

The computed steady-state flow and thermal field in a partially open cavity with a heat source located at the middle of the bottom boundary for various opening heights are examined in this section. To illustrate the effect of opening height on the flow, the following three cases are considered:

- Case A with  $h_0 = 0.8$
- Case B with  $h_0 = 0.5$
- Case C with  $h_0 = 0.3$

For each case under consideration, the opening height, and the strength of the heat source, which is represented by the Grashof number, are varied over a wide range ( i.e.  $10^8 - 10^{15}$ ). As pointed out earlier, it is very difficult to simulate case C ( $h_0 = 0.3$ ) for  $Gr > 10^{11}$ , because of the strong thermal stratification generated inside the cavity. Oscillations develop and make the achievement of steady state very difficult. These oscillations are due to internal gravity waves, and was discussed in greater detail by Abib & Jaluria (1992a, 1992b).

To view qualitatively the effect of opening height on the flow and on the thermal field, contour plots of the stream function, the temperature and the turbulence quantities are presented. This is followed by a detailed discussion of the mean velocity, temperature, turbulent kinetic energy and turbulent eddy diffusivity profiles. Other variables of interest, such as heat transfer and mass flow rates, hot-cold interface height, and stratification level are also given to highlight the effects of opening height on the flow in a partially open cavity. The results for  $Gr = 10^{12}$  are used as an example, since other values of  $Gr$  indicate similar trends. However, when differences arise due to a variation in  $Gr$ , these are pointed out.

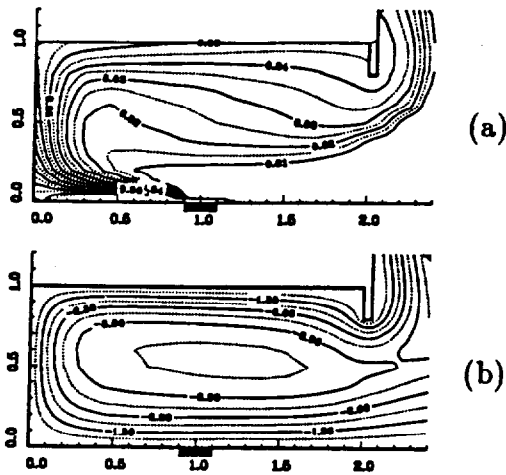


Figure 2: Case A: Steady state turbulent flow and thermal field, at  $Gr = 10^{12}$ , in a partially open cavity with opening height  $h_0 = 0.8$ . (a) Isotherms and (b) Streamlines.

### Flow and Thermal Fields

The steady-state flow and the corresponding thermal fields for a cavity with various opening heights are shown in Figs. 2 - 4, corresponding to the opening height of  $h_0 = 0.8, 0.5$ , and  $0.3$ , respectively. In these figures the isotherms<sup>1</sup> are presented in the top graph (a), while the streamlines<sup>2</sup> are presented in the bottom graph (b).

Cases A and B (with opening height of  $0.8$  and  $0.5$ , respectively) have similar flow patterns as shown in Fig. 2(b) and Fig. 3(b). The only difference is that the flow is more vigorous in case A, because a larger opening is less restrictive to the flow. The flow field reveals the presence of a strong cold floor jet, a hot ceiling jet, and a recirculation region in the middle. The recirculation region is found to increase in size as the opening height is decreased. For a full opening ( $h_0 = 1$ ), a recirculation region does not arise in the cavity.

The isotherms for cases A and B have also a similar pattern as indicated in Fig. 2(a) and Fig. 3(a). However, the temperature level in case B ( $h_0 = 0.5$ ) is much higher due to the larger fluid entrapped in the top region of the cavity. In both cases the walls and the ceiling heat up and the surface temperature rise until a steady state is reached. This temperature rise of the back wall causes a pressure imbalance between the cavity and surrounding ambient medium outside the opening, which forces the vertically rising plume to be drawn toward the wall. This phenomena is the natural convection equivalent of the Coanda effect (Reba 1966) and has received a considerable attention in recent years (Pera

<sup>1</sup>Temperature contours are scaled by a factor of 100 in order to plot legible labels on the plots.

<sup>2</sup>Stream function is scaled by a factor of 1000 for the same reason as above.

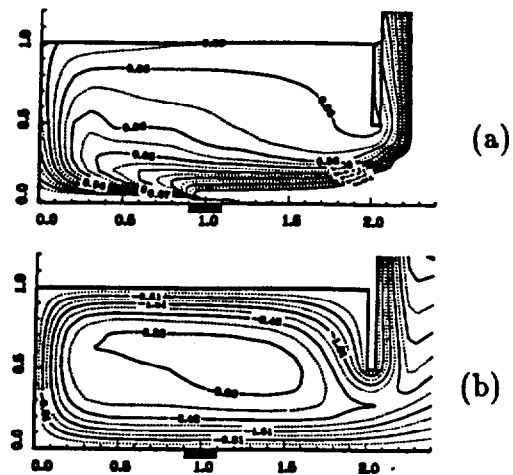


Figure 3: Case B: Steady state turbulent flow and thermal field, at  $Gr = 10^{12}$ , in a partially open cavity with opening height  $h_0 = 0.5$ . (a) Isotherms and (b) Streamlines.

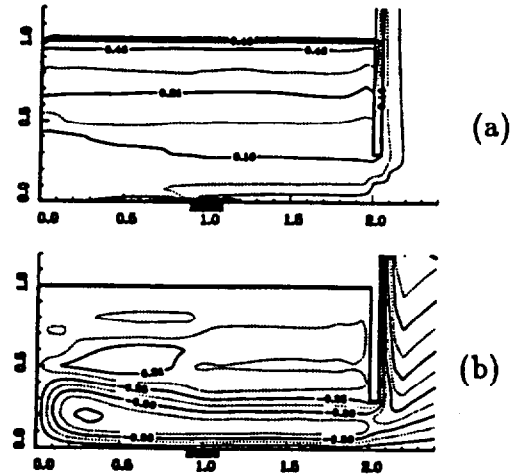


Figure 4: Case C: Steady state turbulent flow and thermal field, at  $Gr = 10^{12}$ , in a partially open cavity with opening height  $h_0 = 0.3$ . (a) Isotherms and (b) Streamlines.

& Gebhart 1975, and Agrawal & Jaluria 1989). Despite the coanda effect, the opening size has no significant influence on the trajectory of the plume.

A completely different flow pattern is observed in case C ( $h_0 = 0.3$ ) as shown in Fig. 4. Because of a smaller opening size, there is a larger volume of fluid trapped in the upper part of the cavity which extends all the way to the door soffit. This upper region or layer becomes stably stratified and almost stagnant. The streamlines in Fig. 4(b) show that the thermal plume penetrates into this large stably stratified region upper layer upto a certain height. As the local buoyancy of the thermal plume decreases, the flow stagnates and then turns away to the right toward the opening. The penetration takes place in the form of a horizontal flow in the

lower part of the stable upper layer. Because of the stratified layer at the upper region of the cavity, the hot-cold interface  $Z_i$  is lowered (see Table 3).

The isotherms in Fig. 4(a) also show that the upper-layer, generated as a result of the heating, is linearly stratified. This stratification is stable because the temperature increases with height and, as a consequence, the turbulence in the upper-layer decays and the flow becomes laminar. This is an example of a circumstance where thermal stratification is generated within the cavity as a result of the interaction between the cavity and the ambient medium outside the opening.

### The Mean Velocity and Temperature

The mean velocity profiles are shown in Fig. 5. The graph shows the  $u$  component variation with  $y$  at several different  $x$  locations, at  $Gr = 1 \times 10^{12}$ , for the three cases: A, B, and C. Again, the mean velocity profiles show that the cases A and B have a similar flow pattern. The flow in case A is slightly more vigorous than that for case B. However, case C is quite different. In Fig. 5, for instance, in case A ( $h_0 = 0.8$ ) the maximum velocity is attained at the opening,  $x = 2.0$ , because the flow is essentially unobstructed. However, in case C ( $h_0 = 0.3$ ) the maximum velocity is not attained at the opening but at a location between the heat source and the back wall. The figure also shows that, in case C, the upper layer is stagnant with the maximum penetration distance of the thermal plume  $\delta p$  equal to 0.55. The penetration distance  $\delta p$  is computed as the maximum vertical distance from the floor to the location where the horizontal component of the velocity  $u$  in the top part of the main (lower) cell becomes zero.

The vertical distribution of the mean temperature is shown in Fig. 6 for the same three cases, at  $Gr \times 10^{12}$ . The figure shows that the mean temperature level rises as the opening height is decreased because of the hot fluid entrapped in the upper region of the cavity. Furthermore, when the opening height is decreased below 0.5, because of entrapped fluid in the upper region, an essentially linear stratification is generated.

Based on the temperature distribution, the cavity can be considered to be divided into a hotter upper layer and cooler lower layer. The hot-cold interface  $Z_i$  is defined as the line of thermal discontinuity separating the hot upper-layer from the cool lower-layer. From plots of the temperature variation along the vertical direction, the height of the hot-cold interface  $Z_i$  can be quantitatively determined. Following Steckler et al. (1982), the height of the interface is estimated from the temperature profile data as the position of rapid temperature change between the lower and the upper portions of the cavity. These temperature profiles illustrate how diffusion and mixing preclude a sharp designation of  $Z_i$ . Consequently, the interface height could only be determined to within  $\pm 10 - 25\%$  accuracy. This interface estimation technique was also used by others including Goldman & Jaluria (1986) and Kapoor & Jaluria (1992).

The height of the interface varies slightly along the  $x$ -

direction. To study the effect of the opening size on the location of the interface, the horizontal location is fixed (i.e., for instance the mid-cavity). The interface  $Z_i$  is given in Table 3 as function of the opening height  $h_0$ . It is seen that, as the opening height is decreased, the temperature level increases indicating a significant lowering of the hot-cold interface. This implies that the hot fluid is recirculated and returns toward the heated area. This result is consistent with the experimental observations of McCaffrey and Quintiere (1977). This lowering of the hot-cold interface has another implication regarding safety. This means that the hot combustion gases and the smoke layer are closer to floor and could prevent, or curb, the fire-fighting and rescue operations.

### Turbulent Quantities

The turbulent quantities such the kinetic energy  $K$  and the turbulent eddy diffusivity  $\nu_t/\nu$  distributions, at  $Gr = 10^{12}$ , are shown in figures Figs. 7 - 9. Again, both  $K$  and  $\nu_t/\nu$  contours show a similar pattern for the opening heights of cases A and B. Most of the turbulence is generated in the thermal plume which becomes attached to the back wall, due to imbalance of pressure between the cavity and the ambient medium (Agrawal & Jaluria 1989), and in the shear layer where the cold inflow and the hot outflow meet. At both of these locations, turbulence production by shear is dominant over that due to buoyancy. Since the temperature gradient is positive, buoyancy production (defined in Eq. 8) is a sink term. In the ceiling area, turbulence is convected by the ceiling jet and, therefore, both  $K$  and  $\nu_t/\nu$  have high values. In mid-cavity, the velocities are low and there is a stable temperature stratification (see Figs. 5-6).

Since the destruction of turbulence by stable gradient depends on the ratio of turbulence reduction due to stratification to turbulence production by shear, this will result in reduction of turbulence and, hence, both  $K$  and  $\nu_t/\nu$  have a low value (cases A and B). The locations of the maximum value of the turbulent kinetic energy  $K_{max}^{1/2} \times Gr^{1/2}$ , for cases A and B, are close to the doorway soffit (see Table 2). This corresponds to the the location of maximum velocity. From the table, it is observed that this location does not vary with  $Gr$ . This is expected physically because, at any given heat input, the location of the maximum velocity is at the doorway soffit where the flow rushes to leave the enclosure.

In case C ( $h_0 = 0.3$ ), the trends are quite different. Turbulence is generated in the thermal plume and the shear layer at the opening. It is convected and diffused throughout the cavity by the recirculating flow. Because of the presence of the strong stable temperature gradient in the upper-layer of the cavity, the turbulence that is convected in the upper-layer is destroyed by this stable gradient. As result, the flow in the upper-layer is relaminarized and turbulence is confined to isolated places, such as the shear layers at the lower left corner (thermal plume attachment to the back wall) and outside the opening (the hot rising wall plume). Unlike the previous cases, A and B, the location

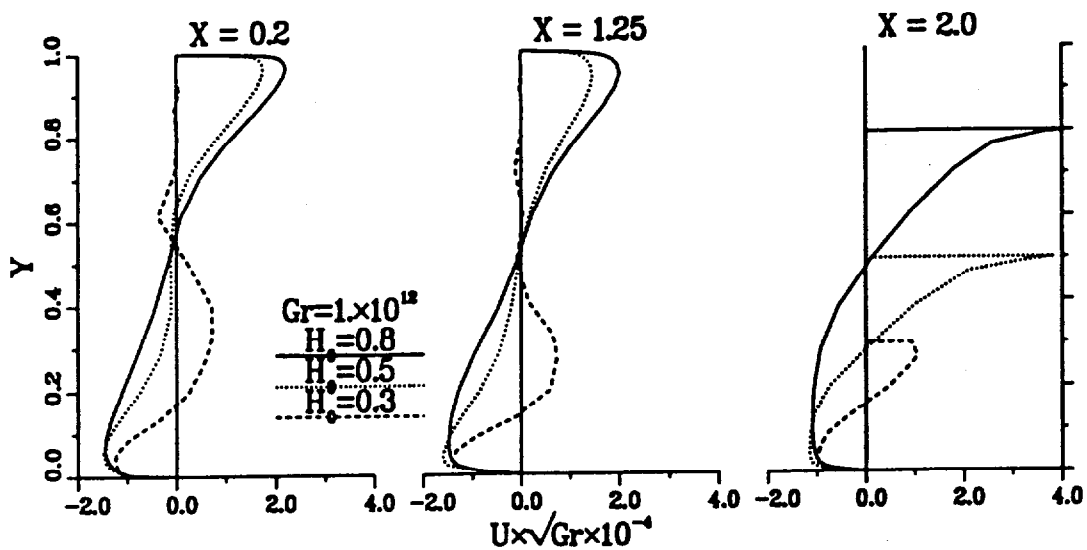


Figure 5: Horizontal component of the mean velocity  $u$  as function of the vertical distance  $y$ , in a partially open cavity with various opening heights, at  $Gr = 10^{12}$ .

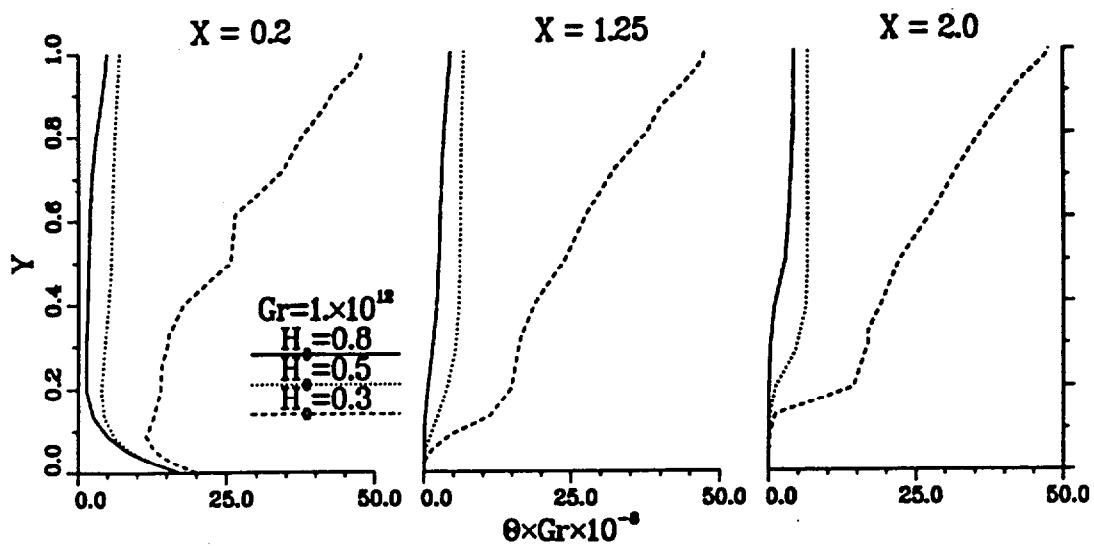


Figure 6: Vertical distribution of the mean temperature  $\Theta$  in a partially open cavity with various opening heights, at  $Gr = 10^{12}$ .

Table 2: Variation of  $K_{max}^{1/2} \times Gr^{1/2}$  with opening height  $h_0$ .

$Gr$	$h_0$		
	0.3	0.5	0.8
$10^9$	166.02 $x = 1.99$ $y = 0.134$	—	—
$10^{10}$	1114.14 $x = 0.799$ $y = 0.022$	1322.5 $x = 1.99$ $y = 0.386$	1680.18 $x = 1.996$ $y = 0.797$
$10^{11}$	2773.8 $x = 0.608$ $y = 0.088$	—	5409.25 $x = 1.998$ $y = 0.797$
$10^{12}$	5386.1 $x = 0.441$ $y = 0.088$	9264.4 $x = 1.99$ $y = 0.479$	13235.2 $x = 1.998$ $y = 0.797$
$10^{13}$	—	13936.3 $x = 1.99$ $y = 0.497$	18606.5 $x = 1.999$ $y = 0.797$
$10^{14}$	—	—	33318.2 $x = 1.986$ $y = 0.797$
$10^{15}$	—	—	86313.4 $x = 1.986$ $y = 0.816$

maximum value of the turbulent kinetic energy for case is near the floor between the source and back wall. As  $Gr$  is increased, the location of  $K_{max}$  shifts toward the back wall. The rise of the thermal plume above the heat source is inhibited by the existence of the stratified upper layer. Therefore, the plume never reaches the ceiling since there is not enough buoyancy to drive it upward. As a consequence, the maximum velocity does not occur at the exit plane but somewhere between the source and back wall.

The cases considered so far are with  $Gr = 10^{12}$ . It is sufficient to say that similar trends exist for other values of  $Gr$ . Of course the flow is more vigorous as  $Gr$  is increased, hence, the turbulence level is higher.

### Turbulent Fluctuations and Eddy Diffusivity Profiles

Profiles of the turbulent kinetic energy  $K$  and of the eddy diffusivity  $\nu_t/\nu$  at  $Gr = 10^{12}$ , are shown in Fig. 10 and Fig. 11. Fig. 10 corresponds to the case A ( $h_0 = 0.8$ ), and shows two peaks in  $K^{1/2}$  and  $\nu_t/\nu$ , one near the boundary-layer at the back wall and the other at the soffit wall. The maximum value of  $K^{1/2}$  and  $\nu_t/\nu$  are located near the exit height of the soffit.

Figure 11 corresponds to case C ( $h_0 = 0.3$ ) and, as explained earlier, shows a trend quite different from the previous case. In Fig. 11, there is only one peak in both  $K^{1/2}$  and  $\nu_t/\nu$  profiles and these are located at the boundary-layer near the back wall. Both  $K^{1/2}$  and  $\nu_t/\nu$  also decrease

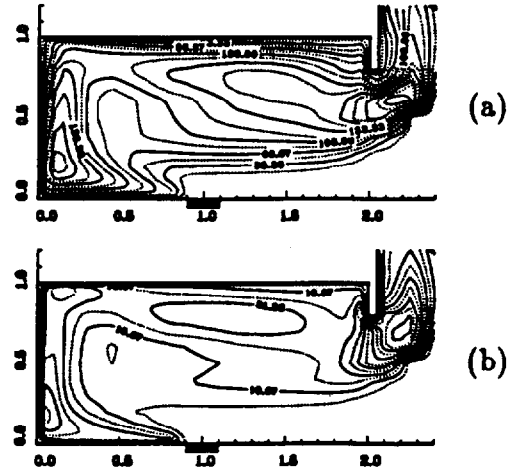


Figure 7: Case A: Contour lines of (a) the turbulent kinetic energy  $K$  and (b) the turbulent eddy diffusivity  $\nu_t/\nu$ , at  $Gr = 10^{12}$ , in a partially open cavity with opening height  $h_0 = 0.8$ .

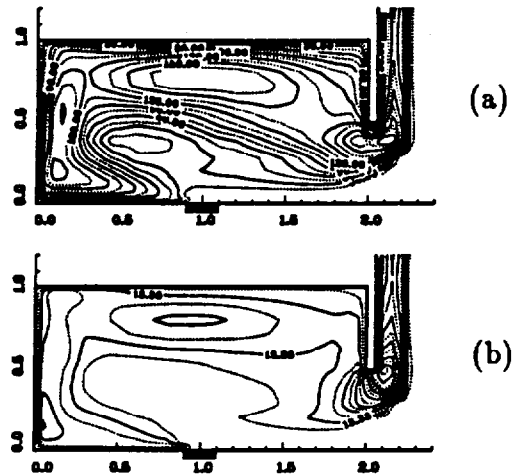


Figure 8: Case B: Contour lines of (a) the turbulent kinetic energy  $K$  and (b) the turbulent eddy diffusivity  $\nu_t/\nu$ , at  $Gr = 10^{12}$ , in a partially open cavity with opening height  $h_0 = 0.5$ .

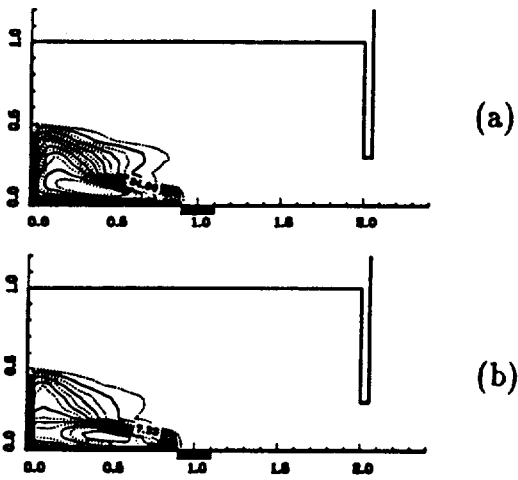


Figure 9: Case C: Contour lines of (a) the turbulent kinetic energy  $K$  and (b) the turbulent eddy diffusivity  $\nu_t/\nu$ , at  $Gr = 10^{12}$ , in a partially open cavity with opening height  $h_0 = 0.3$ .

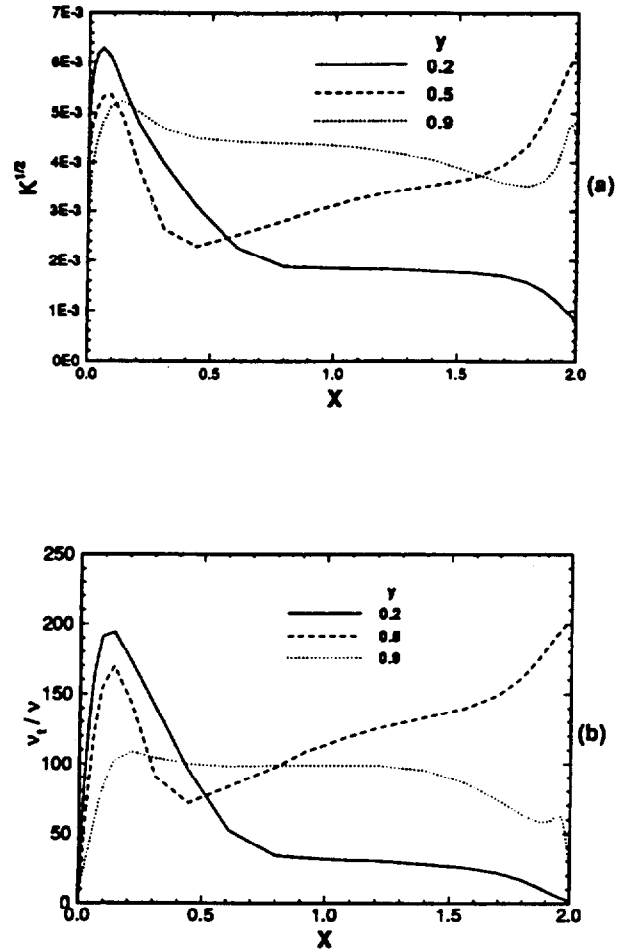


Figure 10: (a) The velocity fluctuation  $K^{1/2}$  and (b) the turbulent eddy diffusivity  $\frac{\nu_t}{\nu}$  profiles, at  $Gr = 10^{12}$ , for a partially open cavity with an opening height  $h_0 = 0.8$ .

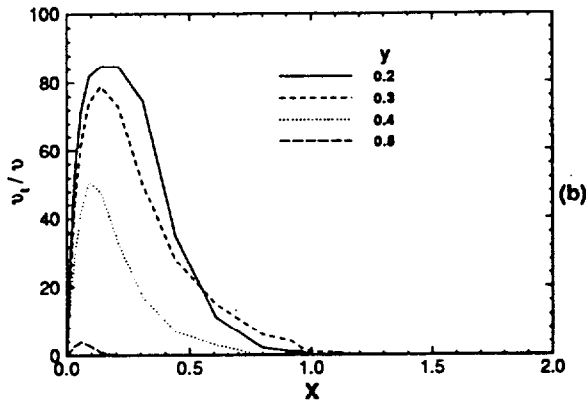
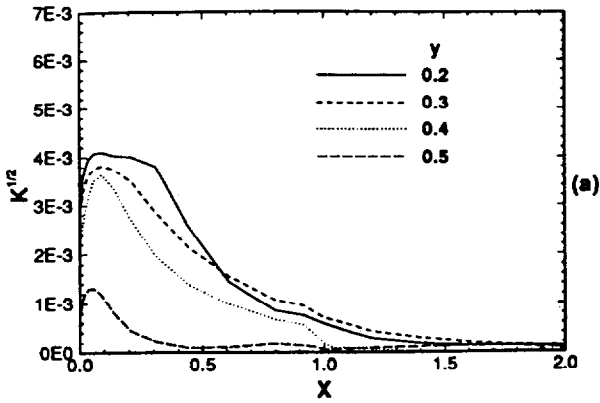


Figure 11: (a) The velocity fluctuation  $K^{1/2}$  and (b) the turbulent eddy diffusivity  $\frac{v_t}{v}$  profiles, at  $Gr = 10^{12}$ , for a partially open cavity with an opening height  $h_0 = 0.3$ .

along the vertical direction due to the presence of the stable stratified layer in the upper part of the cavity. This disappearance of the second peak at the soffit wall is due to the inability of the plume to penetrate into the upper-layer and form a ceiling jet as in the case where the ambient medium is not stably stratified (Quintiere, 1984).

### Mass Outflow and Heat Transfer Rates

The heat transfer rate at the source surface, in terms of a Nusselt number defined as

$$\overline{Nu} = \frac{\bar{h}H}{\kappa} = \frac{1}{l_s^2} \int_0^{l_s} \frac{1}{\Theta_s} dx \quad (17)$$

and the mass outflow rate are two important engineering output variables. The Nusselt number characterizes the surface temperature level or the energy loss/gain at the surface depending on the nature of the boundary conditions. The mass flow rate is an indication of the amount of ventilation

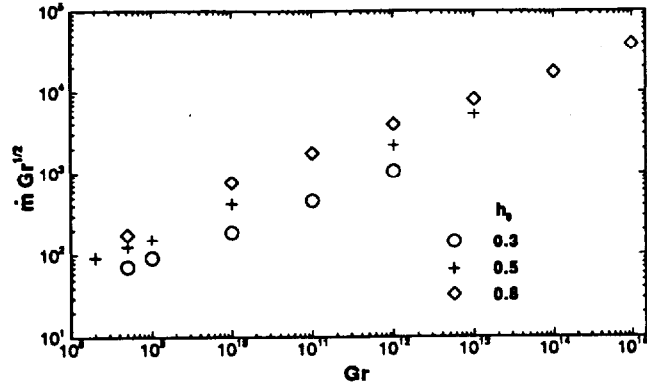


Figure 12: Average mass outflow rate  $\dot{m} \times Gr^{1/2}$  versus  $Gr$  for a partially open cavity with different opening heights.

in the enclosure. The effect of opening height on the mass flow rate and the heat transfer rate for turbulent flow in a partially open cavity, is examined. These results are compared with the available experimental data in the literature.

The mass outflow rate versus  $Gr$  is plotted in Fig. 12 for different opening heights. It shows an increasing flow rate with  $Gr$  and with the opening height  $h_0$ . A least squares curve fit is performed on the numerical data and the following correlation is obtained for mass outflow rate as function of  $Gr$  and opening height  $h_0$ ,

$$\dot{m}\sqrt{Gr} = 0.211 h_0^{1.21} Gr^{0.36} \quad (18)$$

The range over which the above correlation is valid is  $Gr = 10^8 - 10^{15}$  and  $h_0 = 0.3 - 1.0$ . Also it spans both laminar and turbulent flow regimes. The computed mass flow rate at the opening computed by Satoh et al. (1984) is given as

$$\dot{m}\sqrt{Gr} \propto h_0^{1.28} Gr^{1/3} \quad (19)$$

Steckler et. al. (1982) give the mass rate as a function of the opening height  $h_0$  as

$$\dot{m}\sqrt{Gr} \propto W h_0^{1.5} \quad (20)$$

where  $W$  is the width of the opening. Despite the disparity among the various results presented, the experimental results of Satoh (1982) for a doorway opening is in fairly good agreement with the present result.

The average heat transfer rate at the source  $\overline{Nu}_s$ , versus  $Gr$  is plotted in Fig. 13 for various opening heights. The figure shows that the curves which correspond to different opening heights collapse into a single curve. This indicates the insensitivity of  $\overline{Nu}_s$ , to the variation in the opening height at higher  $Gr$ . This occurs because the flow and the heat transfer are very vigorous and, therefore, the effect due to the variation in the opening size is negligible in comparison to the effects due to an increase in the heat input.

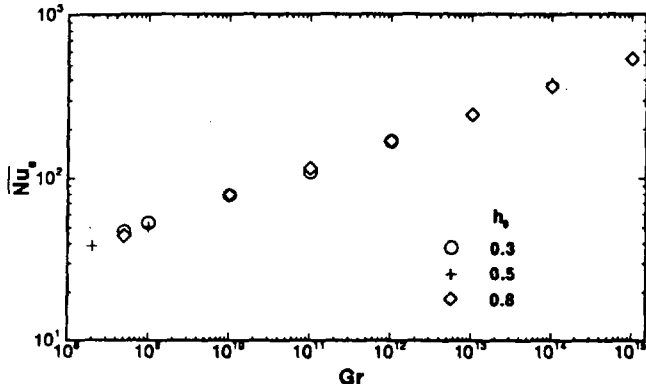


Figure 13: Average Nusselt number  $\overline{Nu}_s$ , versus  $Gr$  for a partially open cavity with different opening heights.

### Maximum Velocity in the Ceiling Jet

The maximum horizontal velocity  $u_{max}$  in the ceiling jet versus  $Gr$  is also plotted in Fig. 14 for various opening heights. This velocity is seen to increase with  $Gr$  as the flow becomes more intense due to an increase in the heat input. A least squares curve fit is performed for  $u_{max}$  in the ceiling jet, yielding the following correlation:

$$u_{max} = 0.623h_0^{1.5}Gr^{0.39}, \quad 10^4 \leq Gr \leq 2 \times 10^8 \quad (21)$$

$$u_{max} = 1.426h_0^{0.6}Gr^{0.36}, \quad 2 \times 10^8 \leq Gr \leq 10^{15}. \quad (22)$$

These equations show that, for higher  $Gr$ , the ceiling jet is a strong function of  $Gr$  and a weak function of the opening height. Regarding the  $Gr$  dependence, the experimental work of McCaffrey and Quintiere (1977) reported  $u_{max}$  (in the ceiling jet) to be proportional to  $Gr^{1/2}$ , while in the present work,  $u_{max}$  is found to vary as  $Gr^{0.36}$ . Alpert's (1971) analytical results of an unobstructed ceiling jet yields  $u_{max} \propto Gr^{1/3}$ . This discrepancy is suspected to be due to 3-D and thermal radiation effects which are neglected in the present work.

### Stratification Level, Penetration Distance, and interface Location

First, attention is focused on the thermal stratification that is generated within the cavity at large  $Gr$  as the opening height is varied. The stratification level  $\gamma$  is obtained by first horizontally averaging the vertical temperature profiles and then taking the slope of the resulting profile which is seen to decrease as the opening height is increased. Table 3 shows the effect of the opening height on the stratification level. At high  $Gr$  (say  $Gr = 10^{12}$ ) a stratified upper-layer is formed. The depth of this layer increases as the opening height is reduced. For  $h_0 = 0.8$  and  $0.5$ , we have an almost linearly stratified upper-layer. The thermal plume rises above the source, gets attached to the back wall and then may or may not reach the ceiling depending on thermal stratification

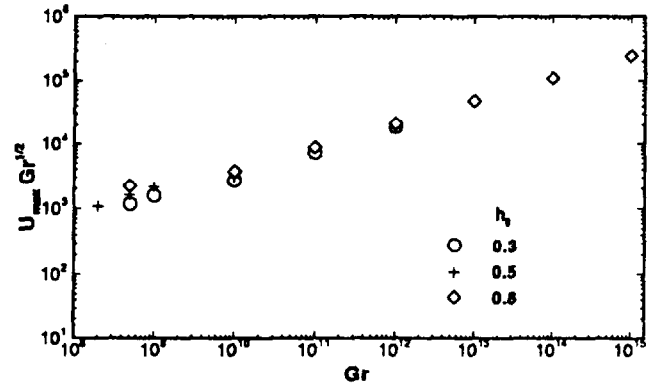


Figure 14: Maximum mean velocity  $u_{max} \times Gr^{1/2}$  versus  $Gr$  in a partially open cavity with different opening heights.

Table 3: Variation of the penetration distance  $\delta p$ , the height of the hot-cold interface  $Z_i$ , and the stratification level  $\gamma$  with the opening height  $h_0$ , at  $Gr = 10^{12}$ .

	$h_0$		
	0.3	0.5	0.8
$\delta p$	0.4	1.0	1.0
$Z_i$	0.4 - 0.15	0.5 - 0.3	0.6 - 0.5
$\gamma$	0.625	0.26	0.2 - 0.1

generated for the given opening height. Table 3 also shows the penetration distance of the plume. It is clear that, in cases A and B, the thermal plume does reach the ceiling. However, for case C, the plume fails to reach the ceiling because of the strong thermal stratification ( $\gamma = 0.65$ ) that is generated within the cavity. The penetration height  $\delta p$  is 0.4 at  $Gr = 10^{12}$ .

The effect of the opening height on the location of the hot-cold interface  $Z_i$  is also given for this case. The location of the interface varies horizontally and so the maximum and the minimum values are also given in the Table 3. The maximum value of  $Z_i$  occurs near the back wall where the wall plume has penetrated the largest in the upper-layer. The minimum value of  $Z_i$  occurs at the door opening where the cold inflow and the hot outflow meet. As seen earlier, case C ( $h_0 = 0.3$ ) is quite different from the two other cases (A and B). This is because of the large linearly stratified layer generated in the top part of the cavity for this case.

Next, the effects of  $Gr$  on the stratification level, penetration distance of the plume and the location of the hot-cold interface for case C (with an opening height of  $h_0 = 0.3$ ) is considered. The results are summarized in Table 4. At

Table 4: Variation of the penetration distance  $\delta p$ , the height of the hot-cold interface  $Z_i$ , and the stratification level  $\gamma$  with  $Gr$  in a partially open cavity with  $h_0 = 0.3$ .

	$Gr$			
	$10^9$	$10^{10}$	$10^{11}$	$10^{12}$
$\delta p$	1.0	0.7	0.5	0.4
$Z_i$	0.5 - 0.4	0.2 - 0.15	0.4 - 0.2	0.4 - 0.15
$\gamma$	0.0	0.35	0.61	0.625

$Gr = 10^9$ , the plume is able to reach the ceiling. Because of mixing due to turbulence and recirculation, a uniform temperature is established in the upper-layer. The stratification level is, therefore, close to zero and the hot-cold interface height  $Z_i$  assumes its highest value for case C ( $Z_i = 0.7$ ). As  $Gr$  is increased to  $Gr = 10^{10}$  the wall plume is unable to reach the ceiling (penetration distance  $\delta p = 0.7$ ) due to the stronger stratification that is generated in the upper-layer ( $\gamma = 0.33$ ). As a result, turbulence is reduced, resulting in less mixing. Because the penetration distance is now decreased, the location of the interface drops downward. As  $Gr$  is further increased to  $10^{11} - 10^{12}$ , the thermal stratification level increases to 0.61 - 0.625 due to the generation of a large stagnant region at the top of the cavity. As a result, the penetration distance and the height of the interface both are found decrease.

## CONCLUSIONS

A numerical study of the two-dimensional turbulent penetrative and recirculating flow induced by localized heating at the bottom surface of a partially open rectangular cavity

is carried out. The background ambient medium is taken as isothermal. The study focuses on the internally generated thermal stratification within the cavity. It is found that thermal stratification can be generated within the partially open cavity, at high  $Gr$ , for relatively small opening heights, in particular, for doorway openings. The height of the generated stratified layer and the corresponding stratification level are expected to increase, at a given  $Gr$ , when the opening height is decreased. Therefore, a behaviour similar to that for stable ambient stratification cases (Abib & Jaluria 1992b) is found to arise. This behavior includes the lowering of the interface  $Z_i$ , between the hot gases and the cold lower region, failure of the thermal plume to penetrate into the stably stratified upper layer generated within the cavity, and decay of turbulence due to the strong stable thermal stratification, and hence, the re-laminarization of the flow in the upper layer of the cavity.

## ACKNOWLEDGMENTS

The authors acknowledge the partial support provided by the Building and Fire Research Laboratory, National Institute of Standards and Technology, under Grant No. 60NANB1H1171 for this work.

## REFERENCES

- Abib, A.H., 1992, "Penetrative and Recirculating Flows in Enclosures with Openings", *Ph.D. Thesis*, Rutgers - The State University of New Jersey, New Brunswick, NJ.
- Abib, A.H., and Jaluria, Y., 1992a, "Penetrative Convection in Partial Open Enclosure", in *Natural Convection in Enclosures - 1992*, ed. Simpkins, P.G., Figliola, R.S., and Georgiadis, J.G., HTD-Vol. 198, pp. 73-81, ASME, New York.
- Abib, A.H., and Jaluria, Y., 1992b, "Turbulent Penetrative and Recirculating Flow in a Compartment Fire", in *Heat and Mass Transfer in Fire and Combustion Systems - 1992*, ed. Cho, P., and Quintiere, J., HTD-Vol. 223, pp. 11-19, ASME, New York
- Agarwal, R. and Jaluria, Y., 1989, "Deflection of a Two-Dimensional Natural Convection Wake Due to the Presence of a Vertical Surface in Close Proximity", *J. Fluid Mech.*, Vol. 201, pp. 35-56.
- Alpert, R.L., 1971, "Fire Induced Turbulent Ceiling Jet", *FMRC Serial No. 197722-2*, Factory Mutual Research Corp., Norwood, Mass.
- Chan, Y.L., and Tien, C.L., 1985, "Numerical Study of Two-Dimensional Laminar Natural Convection in Shallow Open Cavities", *Int. J. Heat and Mass Transfer*, Vol. 28, pp. 603-612.
- Davidson, L., 1990, "Calculation of the Turbulent Buoyancy-driven Flow in a Rectangular Cavity Using an Efficient Solver and Two Different Low Reynolds  $k-\epsilon$  Turbulence Models", *Numerical Heat Transfer, Part A*, Vol. 18, pp. 129-147.
- Emmons, H.W., 1973, "Natural Convective Flow Through an Opening", *Part I, Home Fire Project Technical Report No. 1*, Harvard Univ., Cambridge, Mass.

- Emmons, H.W., 1978, "The Prediction of Fire in Buildings", *17th Symp. (int.) Combustion*, Combustion Institute, pp. 1101.
- Fraikin, M.P., Portier, J.J., and Fraikin, C.J., 1980, "Application of a  $k-\epsilon$  Turbulence Model to an Enclosed Buoyancy Driven Recirculating Flow", *ASME-AIChE Nat. Heat Transfer Conference*, Paper No. 80-HT-68.
- Goldman, D, and Jaluria, Y., 1986, "Effect of Opposing Buoyancy on the Flow in Free and Wall Jet", *J. Fluid Mech.*, Vol. 166, pp. 41-56.
- Kapoor, K. and Jaluria, Y., 1992, "Penetrative Convection of a Plane Turbulent Wall Jet in a Two-layer Thermally Stratified Environment", to appear in *Int. J. Heat Mass Transfer*.
- Kawagoe, K., 1958, "Fire Behavior in Rooms", *Rep. 27*, Building Research Institute, Japan.
- Kettleborough, C.F., 1972, "Transient Laminar Free Convection Between Heated Vertical Plates Including Entrance Effects", *Int. J. Heat and Mass Transfer*, Vol. 15, pp. 883-896.
- Ku, A.C., Doria, M.L., Lloyd, J. R., 1976, "Numerical Modeling of Buoyant Flows Generated by Fire in a Corridor", *Proc. 16th Symp. (int.) on Combustion*, Combustion Institute, pp. 1372-1384.
- Lam, C.K.G. and Bremhorst, K., 1981, "A Modified Form of the  $k-\epsilon$  Model for Predicting Wall Turbulence", *J. Fluid Engng*, Vol. 13, pp. 456-460.
- Lauder, B.E., and Spalding, D.B., 1974, "The Numerical Computation of Turbulent Flows", *Comput. Meth. Appl. Mech. Eng.*, Vol. 3, pp. 269-289.
- Le Quere, P., Humphrey, J.A.C., and Sherman, F.S., 1981, "Numerical Calculation of Thermally Driven Two-Dimensional Unsteady Laminar Flow in Cavities of Rectangular Cross Section", *Numerical Heat Transfer*, Vol. 4, pp. 249-283.
- Markatos, N.C., Malin, M.R., and Cox, G., 1982, "Mathematical Modeling of Buoyancy-Induced Smoke Flow in Enclosures", *Int. J. Heat Mass Transfer*, Vol. 25, pp. 63-75.
- Markatos, N.C. and Cox, G., 1982, "Turbulent Buoyant Heat Transfer in Enclosures Containing a Fire Source", *17th Int. Heat Transfer Conference*, Vol. 6, pp. 373.
- McCaffrey, B.J., and Quintiere, J.G., 1977, "Buoyancy Driven Countercurrent Flow Generated by a Fire Source", in Spalding, D.B., and Afgan, N. (Eds.), *Heat Transfer and Turbulent Buoyant Convection*, Vol. II, pp. 457-472, Hemisphere, Publishing Corp., New York.
- Patankar, S.V., 1980, *Numerical Heat Transfer and Fluid Flow*, Hemisphere, Washington, D.C.
- Penot, F., 1982, "Numerical Calculation of Two-Dimensional Natural Convection in Isothermal Open Cavities", *Numerical Heat Transfer*, Vol. 5, pp. 421-437.
- Pera, L. and Gebhart, B., 1975, "Laminar Plume Interactions", *J. Fluid Mech.*, Vol. 68, pp. 259-271.
- Prahl, J. and Emmons, H.W., 1975, "Fire Induced Flow Through an Opening", *Combustion and Flame*, Vol. 25, pp. 369-385.
- Quintiere, J.G., 1977, "Growth of Fire in Building Compartments", in Robertson, A.F., (Ed.), *Fire Standards and Safety*, ASTM STP 614, American Soc. for Testing and Materials, pp. 131-167.
- Quintiere, J.G., 1981, "An Approach to Modeling Wall Fire Spread in a Room", *Fire Safety Journal*, Vol. 3, pp. 201-214.
- Quintiere, J.G., 1984, "Perspective on Compartment Fire Growth", *Combust. Sci. Technol.*, Vol. 39, pp. 11-54.
- Reba, I., 1966, "Application of the Coanda Effect", *Scientific American*, Vol. 214, No. 6, pp. 84-92.
- Roache, P.J., 1972, *Computational Fluid Dynamics*, Hermosa Publishers, Albuquerque, New Mexico.
- Rockett, J.A., 1976, "Fire Induced Gas Flow in an Enclosure", *Combustion Science and Technology*, Vol. 12, pp. 165-175.
- Rodi, W., 1980, "Turbulence Models and Their Application in Hydraulics, a State of the Art Review", *International Association for Hydraulics Research*, Delft, The Netherlands.
- Satoh, K., Lloyd, J.R., Yang, K.T., and Kanury, A.M., 1983, "A Numerical Finite-Difference Study of the Oscillatory Behavior of Vertically Vented Compartments", in Shih, T.M. (Ed.), *Numerical Properties and Methodologies in Heat Transfer*, Hemisphere, New York, NY, pp. 517-528.
- Satoh, K., 1982, "An Approach to Modeling of Aircraft Cabin Fire Phenomena - The Ventilation Effect of Location and Geometry of the Heat Source and Opening in an Aircraft Passenger Cabin", *Report of Fire Research Institute*, Japan, No. 53, pp. 43.
- Satoh, K., Lloyd, J.R. and Yang, T.K., 1984, "A Numerical Study of a Buoyant Flow in Enclosures with Vertical Openings - Effect of Heat Source and Opening Locations", *ASME Nat. Heat Transfer Conf.*, Buffalo, NY, pp. ?
- Simcox, S., Wilkes, N.S., and Jones, I.P., 1989, "Computer Simulation of the Flow of Hot Gases from the Fire at King's Cross Underground Station", *Proc. Symp. King's Cross Underground Fire*, pp. 19-25, London: Inst. Mech. Eng.
- Steckler, K.D., Quintiere, J.G. and Rinkinen, W.J., 1982, "Flow Induced by Fire in a Compartment", *19th Symp. (Int.) Combustion*, Combustion Institute, pp. 913-920.
- Steckler, K.D., Rehm, H.R. and Quintiere, J.G., 1984, "Fire Induced Flows Through Room Openings - Flow Coefficients", *20th Symp. (Int.) Combustion*, Combustion Institute, pp. ?
- Thom, A., 1928, (Cited in Roache, 1972), "An Investigation of Fluid Flow in Two Dimensions", *Aerospace Research Center, R. and M.*, No. 1194, United Kingdom.
- Thomas, P.H., Heselden, A.J.M. and Law, M., 1967, "Fully-Developed Compartment Fires - Two Kinds of Behaviour", *Fire Research Tech. Paper No. 18*, Fire Research Station, Borehamwood, UK.
- Zukoski, E.E., 1975, "Convective Flows Associated with Room Fires", *Semi-Annual Progress Report, NSF GI 31892XI*, California Institute of Technology, Pasadena, CA.
- Zukoski, E.E., and Kubota, T., 1978, "A Computer Model for Fluid Dynamic Aspects of a Transient Fire in a Two Room Structure", *DOC NBS Grant No. 5-9004*, Cal. Inst. Technol., Pasadena, CA.